Industrial Crops & Products 182 (2022) 114870

Contents lists available at ScienceDirect

Industrial Crops & Products

journal homepage: www.elsevier.com/locate/indcrop

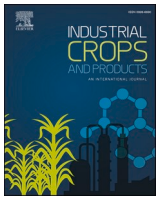

Vegetable oil-based, coumarin-containing antibacterial thermosets with improved thermal stability via copper-free thermal azide-alkyne click polymerization

Emrah Çakmakçı [a,*], Mücahit Özdemir [a], Ferhat Şen [b], Mustafa Bulut [a], Bahattin Yalçın [a]

[a] Marmara University, Göztepe Campus, Department of Chemistry, Faculty of Science and Literature, 34722 Istanbul, Turkey
[b] Zonguldak Bülent Ecevit University, Department of Food Processing, 67900 Zonguldak, Turkey

ARTICLE INFO

Keywords:
Castor oil
Dimer diamine
Azide-alkyne click reaction
Phosphorus
Coumarin
Antibacterial

ABSTRACT

In recent years, the preparation of thermoset materials based on renewable sources has received peculiar attention. In this work, we prepared vegetable oil based antibacterial thermosets via thermal azide−alkyne cycloaddition reactions. Dimer diamine was propargylated and mixed with azidated trimethylolpropane triglycidyl ether and castor oil bearing azide and phosphorous groups. Two different propargyl functionalized coumarins were also incorporated into the vegetable oil based formulations. All synthesized monomers were characterized by Fourier-transform infrared (FTIR) and Nuclear magnetic resonance (NMR) spectroscopy. Mechanical, thermal and antibacterial properties of the obtained thermosets were also determined. The thermosets behaved as elastomers and displayed elongation at break values between 39% and 82%. The phosphorylated castor oil derivative improved the thermal properties and char yields as high as 13.83% at 750 °C were observed under nitrogen atmosphere. Coumarin-containing thermosets were found to have antibacterial activity against both gram-positive and gram-negative bacteria.

1. Introduction

Due to the environmental concerns in petroleum-based products and the accelerated depletion of petroleum resources brought by the increasing population and by the rapid consumption caused by technological developments, researchers have turned to more sustainable systems using renewable resources (Ma et al., 2013; Besset et al., 2010; Pansumdaeng et al., 2020; Auvergne et al., 2014; Gandini and Lacerda, 2015).

In recent years, many bio-based materials have been reported for a wide range of applications which were prepared by using environmental-friendly building blocks such as isosorbide (Cakmakci et al., 2019), vegetable oils (Mülazim et al., 2011), vanillin (Harvey et al., 2015), lignin (Çalgeris et al., 2012), eugenol (Chen et al., 2019; Chen et al., 2019), pyrogallol (Uemura et al., 2016), etc. Among these renewable sources, vegetable oils are widely studied and utilized due to their low cost and high abundance (Alam et al., 2014; Alam and Alandis, 2014). Besides, the presence of various functional groups such as ester linkages, double bonds, allylic hydrogens, and hydroxyl groups (depending on the nature of the fatty acids) in vegetable oils, make them highly attractive for a wide range of different modifications (Şeker and Çakmakçi, 2020).

Click reactions that give high yields with a low amount of side product formation, are modular, simple, effective, and environmental-friendly. Thus, click reactions are fascinating tools in modern chemistry in terms of Green Chemistry (Tunca, 2018; Tasdelen and Yagci, 2013; Kolb et al., 2001; Hoyle et al., 2010; Fernández-Francos et al., 2016; Arévalo et al., 2016; Gupta et al., 2020). Click chemistry protocols have been widely used for the modification of bio-based building blocks and the synthesis of polymers therefrom. For instance, various functional groups such as carboxylic acid, hydroxyl, isocyanate, epoxy, amine, etc., were introduced with ease to vegetable oils via thiol-ene click reactions for a broad spectrum of applications (Ionescu et al., 2015; He et al., 2014; Feng et al., 2017). Another useful tool within the palette of click chemistry is the azide-alkyne cycloaddition reaction which is a type of Huisgen 1,3-dipolar cycloaddition and previously it was utilized for the preparation of various bio-based materials (Singh et al., 2016; Han et al., 2016; Xu et al., 2016; Besset et al., 2010). Generally copper-based metal catalysts are required for this type of click reaction, however, these reactions can also be conducted by heating in the absence of a catalyst

* Corresponding author.
E-mail address: emrah.cakmakci@marmara.edu.tr (E. Çakmakçı).

https://doi.org/10.1016/j.indcrop.2022.114870
Received 31 December 2021; Received in revised form 23 March 2022; Accepted 25 March 2022
Available online 1 April 2022

(Besset et al., 2010; Lutz, 2008). The latter route; thermal azide−alkyne cycloaddition (TAAC) is an intriguing strategy to prepare sustainable polymers from vegetable oils due to its straightforward and benign reaction conditions. For instance; Hong et al. (2013) showed that azidated vegetable oil can be crosslinked with different diynes to give polymers that exhibit different characteristics such as rubber-like, brittle or tough plastics. In another work Yuan et al. (2018) prepared elastomers via TAAC by using alkyne-functionalized lignin and azide-functionalized soybean oil-based acrylic polymers. The prepared elastomers exhibited excellent elasticity with tensile strain percentages over 110%.

In this work, we aimed to prepare antibacterial and thermally stable thermoset materials from vegetable oils via TAAC. We first synthesized a tetra-propargyl functionalized dimer diamine oligomer. Dimer diamines are low viscosity and hydrophobic building blocks which are synthesized by the Diels−Alder reaction of fatty acids. They bring flexibility and impact resistance when used in coatings (Froidevaux et al., 2016). As for the azide component, we used azidated trimethylolpropane triglycidyl ether (ATMPTGE) and castor oil (CO). We found an elegant way to introduce both azide and phosphorous groups (for thermal stability) to CO. Next, we incorporated two novel propargyl functionalized coumarin derivatives for antibacterial activity. Coumarins which are naturally occurring substances in many plants are useful platforms for the synthesis of antibacterial agents, photosensitizers, drugs and several organic molecules for different applications (Borges et al., 2005; Abdallah et al., 2019; Zhang et al., 2016; Chen et al., 2019; Chen et al., 2019). We characterized all synthesized oligomers and monomers by FTIR and NMR spectroscopy. We measured the mechanical and thermal properties of the obtained thermosets as well as their antibacterial properties.

2. Experimental

2.1. Materials

2,4-Dihydroxybenzaldehyde, salicylaldehyde, phenylacetic acid, 4-hydroxyphenylacetic acid, propargyl bromide, potassium carbonate, propargyl acrylate (PA), phosphorus(V) oxychloride ($POCl_3$), castor oil (CO), bromoethanol, anhydrous sodium sulfate, triethyl amine (TEA), ammonium chloride, trimethylolpropane triglycidyl ether, sodium chloride, dichloromethane (CH_2Cl_2), methanol, diethyl ether, and *N*,*N*-dimethylformamide (DMF) were all purchased from Sigma Aldrich and used as received. Dimer diamine (PRIAMINE 1071 by Croda, its theoretical molecular weight is 547 g/mol and its amine number is 205 mg KOH/g) was obtained as a gift from MCT chemicals (Turkey). Azidoethanol (Daglar et al., 2021) and ATMPTGE (Kargarfard et al., 2018) were synthesized according to the literature. S. aureus and E. coli were obtained from a local company.

2.2. Characterization Methods

Fourier-Transform Infrared Spectroscopy (FTIR) spectra were recorded on a Shimadzu FTIR 8300 spectrometer with ATR capability. ^{1}H NMR (500 MHz) spectra were recorded using an Agilent VNMRS 500 instrument in $CDCl_3$. Elemental analyses carried out using a LECO CHN 932 were performed by the Instrumental Analysis Laboratory of the Tubitak Marmara Research Center. Gel content values were determined via soxhlet extraction with CH_2Cl_2 for 6 h. Thermal gravimetric analysis (TGA) was carried out using thermal data were obtained by using the Perkin Elmer Diamond Thermal Analysis instrument. The TGA measurements were performed between 30 °C and 750 °C (under N_2, rate 10 °C/min). Differential scanning calorimetry (DSC) experiments were performed under a nitrogen atmosphere on the Perkin Elmer Pyris Diamond DSC apparatus. Samples were kept at − 50 °C for 2 min and then heated to 50 °C with a heating rate of 20 °C/min. After holding 2 min at this temperature, samples were cooled to − 50 °C with a cooling rate of 50 °C/min, followed by keeping at this temperature for 2 min. Finally, they were reheated to 50 °C with a heating rate of 20 °C/min. Data from the second heating cycle were reported. Mechanical properties of the thermosets were determined by standard tensile stress-strain tests to measure modules, ultimate tensile strength and elongation at break. Standard tensile stress-strain experiments were performed at room temperature on a Materials Testing Machine Z010/TN2S, with a crosshead speed of 2 mm/min.

Antibacterial tests were conducted according to our previous publications (Cakmakci et al., 2019; Şen and Kahraman, 2018; Birtane et al., 2021; Şen et al., 2017; Beyler-Çiğil et al., 2021).

2.3. Synthesis of propargylated coumarins

The precursors; 7-hydroxy-3-phenyl-coumarin and 3-(4-hydroxyphenyl)-coumarin were synthesized according to the literature (Hu et al., 2019).

2.3.1. 3-[4-(Prop-2-yn-1-yloxy)phenyl]-coumarin (PPC)

3.00 g (12.6 mmol) 3-(4-hydroxyphenyl)-coumarin and 1.50 g (12.6 mmol) propargyl bromide were dissolved in 30 mL DMF solution at argon atmosphere. 2.61 g (18.9 mmol) potassium carbonate was added slowly, and the reaction was stirred overnight at 65 °C. Then, the reaction mixture was poured into the ice water. The precipitated product was filtered and dried under vacuum. The crude product was purified by column chromatography on silica gel using chloroform as eluent.

Yield 3.44 g (99.0%). Mp:182 °C. Anal. calcd. for $C_{18}H_{12}O_3$: C, 78.25; H, 4.38%; found: C, 78.28; H, 4.39%. FTIR (ATR): υ_{max}, cm^{-1}: 3285 (C≡C–H), 3062 (Ar–CH), 2942–2865 (Aliphatic–CH), 2118 (C≡CH), 1710 (C═O), 1608 (Ar–C═C). ^{1}H NMR (D-$CDCl_3$, 500 MHz, δ, ppm): 7.80 (s, 1 H), 7.73 – 7.70 (m, 1 H), 7.56 – 7.53 (m, 2 H), 7.39 (d, J = 8.2 Hz, 2 H), 7.31 (d, J = 6.2 Hz, 1 H), 7.09 – 7.07 (m, 2 H), 4.76 (d, J = 3.6 Hz, 2 H), 2.56 (d, J = 4.9 Hz, 1 H).

2.3.2. 3-Phenyl-7-(prop-2-yn-1-yloxy)-coumarin (PC)

3.00 g (12.6 mmol) 7-hydroxy-3-phenyl-coumarin and 1.50 g (12.6 mmol) propargyl bromide were dissolved in 30 mL DMF solution at argon atmosphere. 2.61 g (18.9 mmol) potassium carbonate was added slowly, and the reaction was stirred overnight at 65 °C. Then, the reaction mixture was poured into the ice water and precipitated. The precipitated product was filtered and dried under vacuum. The crude product was purified by column chromatography on silica gel using chloroform as eluent.

Yield 3.48 g (100%). Mp: 138 °C. Anal. calcd. for $C_{18}H_{12}O_3$: C, 78.25; H, 4.38%; found: C, 78.26; H, 4.40%. FTIR (ATR): υ_{max}, cm^{-1}: 3280 (C≡C–H), 3061 (Ar–CH), 2936–2870 (Aliphatic–CH), 2121 (C≡CH), 1714 (C═O), 1610 (Ar–C═C). ^{1}H NMR (D-$CDCl_3$, 500 MHz, δ, ppm): 7.80 (d, J = 4.8 Hz, 1 H), 7.73 – 7.69 (m, 1 H), 7.46 (tt, J = 14.9, 7.4 Hz, 5 H), 6.99 (dt, J = 27.4, 6.9 Hz, 2 H), 4.80 (d, J = 5.0 Hz, 2 H), 2.60 (d, J = 9.1 Hz, 1 H).

The synthesis of PC and PPC are presented in Scheme 1.

2.4. Synthesis of propargylated dimer diamine (PDD)

PDD was obtained via the aza-Michael reaction of dimer diamine with PA. 5.47 g of dimer diamine (10 mmol) was dissolved in 20 mL of methanol in a one-neck round bottom flask equipped with a dropping funnel. The flask was immersed into an ice bath at 0 °C. Then 4.62 g of PA (10.5 mmol, 1.05 times excess) was added to the flask drop by drop within 30 min under stirring. The mixture was kept at 0 °C for 1 h after the addition and then stirred overnight at room temperature. The unreacted PA and methanol were all removed via rotary evaporator under vacuum. PDD was obtained as a yellowish viscous liquid. The synthesis of this tetra alkyne functional oligomer is depicted in Scheme 2.

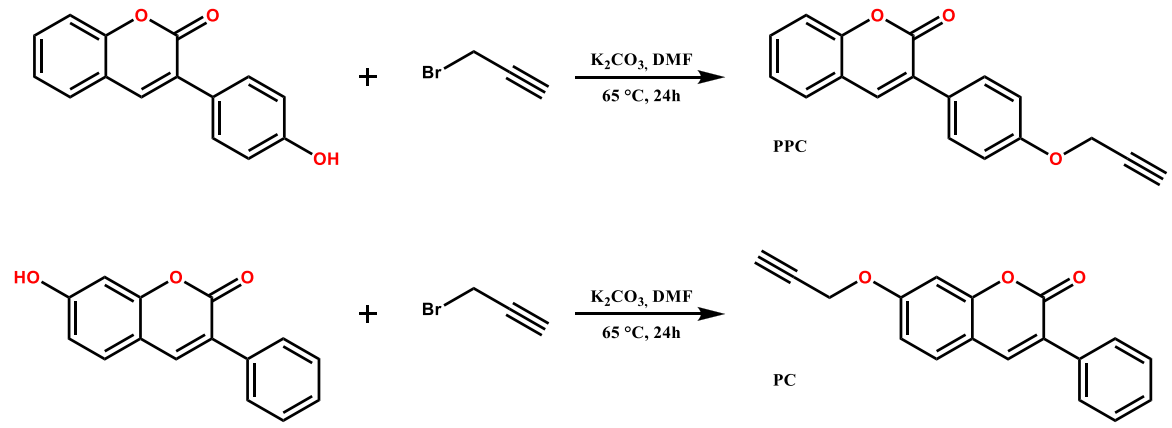

Scheme 1. The general synthesis scheme of the new coumarins bearing propargyl group.

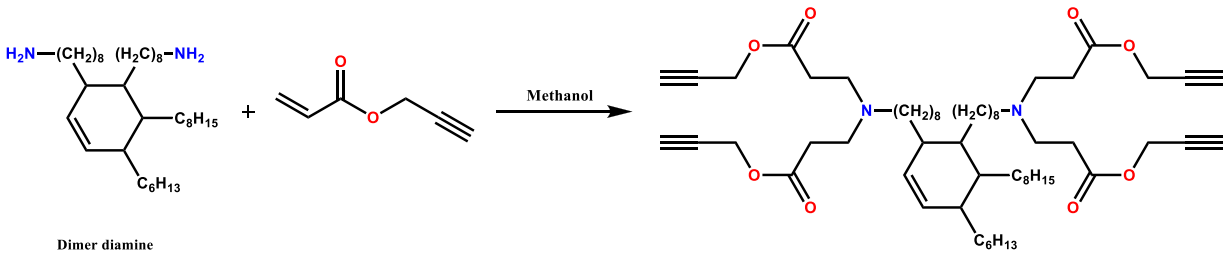

Scheme 2. Synthetic route to propargylated dimer diamine (PDD).

2.5. Synthesis of PAMCO

Phosphorous and azide bearing castor oil derivative (PAMCO) was synthesized in two steps in one pot. In the first step 10.00 g of CO (28.6 mmol OH), 30 mL of CH_2Cl_2 and 3.04 g of TEA were transferred to a three-neck round bottom flask equipped with a dropping funnel, a gas inlet (N_2) and a condenser. The flask was placed in an ice bath at 0 °C. 4.60 g of $POCl_3$ (30 mmol) was dissolved in 20 mL of CH_2Cl_2 and then added to the CO solution dropwise within an hour under stirring and nitrogen atmosphere. The solution was stirred at 0 °C for an additional of 1 h after the addition was completed then further stirred for 4 h at room temperature. In the second step, the flask was immersed into another ice bath again and a mixture of 5.22 g of azidoethanol (60 mmol), 6.07 g of TEA and 20 mL of CH_2Cl_2 was added dropwise to this mixture within 1 h. Then the solution was left to stir overnight. CH_2Cl_2 was removed via rotary evaporator and then 50 mL of diethyl ether was added. The precipitated, undissolved salts were removed via filtration. The organic phase was washed with brine (3 ×20 mL) and distilled water (3 ×20 mL), respectively. The organic phase was separated, dried over anhydrous sodium sulfate and after filtration, the ether was evaporated under vacuum. The obtained yellow oil was kept in a refrigerator. The structure of PAMCO is illustrated in Scheme 3.

2.6. Preparation of cured thermosets via TAAC

The thermoset materials were obtained via TAAC. A 1:1 azide to alkyne ratio was maintained in the reactions. Required amounts of PAMCO, PDD, ATMPTGE and propargylated coumarins (Table 1) were weighed and a sufficient amount of DMF was added to dissolve all the monomers. The obtained viscous solutions were poured into Teflon molds. The molds were first heated to 65 °C for 16 h in a vacuum oven. Then the films were kept for one hour at 85 °C and 100 °C, respectively and finally the heating was continued for 6 h at 120 °C under vacuum. Yellow/orange or brown/black colored films (Fig. 1) were obtained after curing.

The TAAC curing of the synthesized monomers is illustrated in Scheme 4. We added the coumarins at 20% and 40% of the total required alkyne mole ratio. The samples were coded as DPA-PCX or DPA-PPCX where D, P and A stand for PDD, PAMCO and ATMPTGE and X stands for the weight percentage of the coumarins.

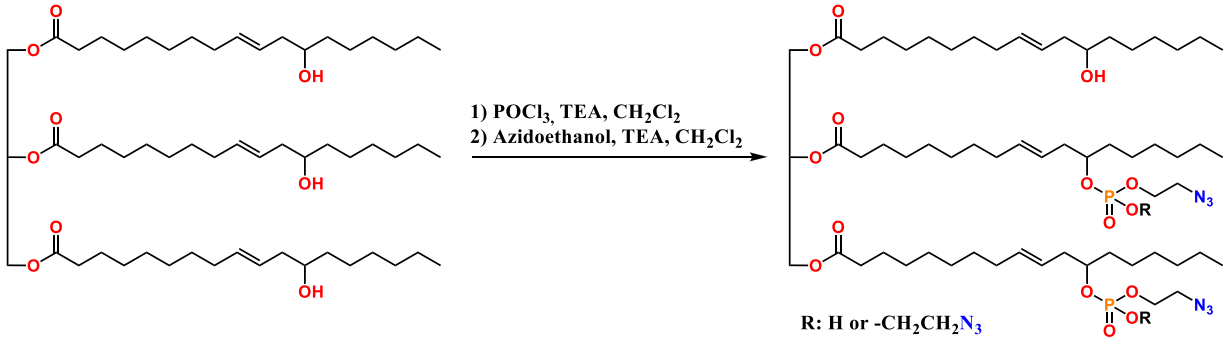

Scheme 3. Synthesis of phosphorous-and azide-modified castor oil.

Table 1
Recipe for the TAAC reactions[a].

	PDD (g)	PAMCO (g)	ATMPTGE (g)	Propargyl coumarin (g)	Propargyl phenylcoumarin (g)
DPA	0.4935 (0.5 mmol)	0.36	0.1528	–	–
DPA–PC10	0.395 (0.4 mmol)	0.36	0.1528	0.1104 (0.4 mmol)	–
DPA–PC20	0.2962 (0.3 mmol)	0.36	0.1528	0.2208 (0.8 mmol)	–
DPA–PPC10	0.395 (0.4 mmol)	0.36	0.1528	–	0.1104 (0.4 mmol)
DPA–PPC20	0.2962 (0.3 mmol)	0.36	0.1528	–	0.2208 (0.8 mmol)

[a] Approximately 0.5 mL of DMF was added to each formulation. PDD's molecular weight was calculated as 987.44 g/mol (547 + 4 ×110.11) and the required amount of PAMCO and ATMPTGE were calculated based on their nitrogen contents determined by elemental analysis.

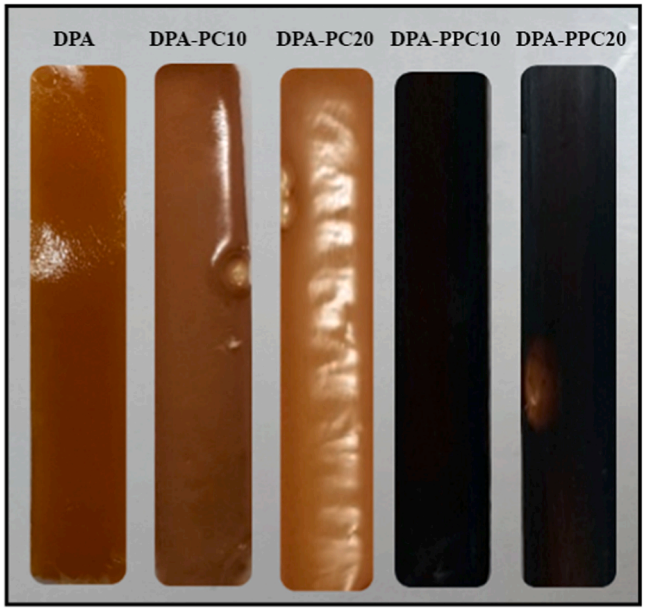

Fig. 1. The digital photographs of the prepared vegetable oil-based thermosets.

3. Results and discussion

3.1. Characterization of the synthesized monomers

The new coumarins bearing propargyl group were synthesized by the nucleophilic substitution reaction at 65 °C temperature and argon atmosphere. Two new coumarins were characterized by spectroscopic methods such as FTIR, ^{1}H NMR, and elemental analysis. Fig. 2 displays the ^{1}H NMR spectra of PC and PPC. The ≡CH protons resonated at around 2.6 ppm while the signals at around 4.80 ppm correspond to the protons on the carbon adjacent to the oxygen. The aromatic protons as well as the characteristic double bond protons of the coumarin ring (–C**H**=C(COO)C) were observed between 7.0 and 8.0 ppm.

The coumarins were further characterized by FTIR spectroscopy (Fig. 3). The vibrational bands associated with the hydroxyl group on starting coumarins vanished from their FTIR spectra, indicating the propargylation of the coumarin derivatives. The formation of the coumarins PC and PPC were indicated by the observation of new alkyne peaks at 3280 cm^{-1} and 2121 cm^{-1} belonging to the vibration of C≡C–H and –C≡C– bonds on these compounds, respectively.

The PDD was synthesized via aza-Michael addition reaction of dimer diamine and PA. PA was taken slightly excess than the required stoichiometry and then at the end of the reaction the excess PA was removed via rotary evaporation and thus PDD was obtained quantitatively. The structure of PDD was characterized by FTIR and ^{1}H NMR spectroscopy. The FTIR spectra of neat dimer diamine, PA and PDD are presented in Fig. 4. The bands at 1610 cm^{-1} and 794 cm^{-1} in the FTIR spectrum of the neat dimer diamine are due to in plane and out of plane bending vibrations of the –NH_2 groups, respectively. The bands between 2920 and 2850 cm^{-1} are due to the –CH stretching vibrations while the bands at 1458 and 1378 cm^{-1} correspond to the scissoring vibrations of –CH_2- and –CH_3 groups. C–N vibration bands were detected at 1076 cm^{-1}. All these findings are in good accordance with the literature (Agnaou et al., 2014). The ≡CH vibrations in PA were detected at 3293 cm^{-1}. The characteristic acrylate double bond bands in PA were observed at 1635 and 807 cm^{-1} in addition to the characteristic ester carbonyl which was detected at 1724 cm^{-1}. After the reaction, as expected, the bands of the acrylate double bonds were disappeared as can be seen from the spectrum of PDD. Moreover, the carbon-hydrogen bond of the alkyne groups (≡CH) was slightly shifted and observed at 3310 cm^{-1}. These results clearly prove that PDD was synthesized successfully.

The structure of PDD was further characterized by ^{1}H NMR spectroscopy. The characteristic aliphatic protons of neat dimer diamine were observed in the range of 0.8–2.00 ppm (Fig. 5). The –CH_2 protons neighbouring the nitrogen (–**CH_2**NH_2) resonated at around 2.67 ppm. Weak NMR peaks were detected at around 5.00–6.00 ppm (are not shown in the spectrum for clarity) belonging to the hydrogens of the alkene double bonds. After modification new peaks appeared in the spectrum of PDD (Fig. 5). The terminal alkyne ≡CH hydrogens resonated at around 2.38 ppm while the –CH_2 groups adjacent to the oxygen were observed at 4.68 ppm. The 12 protons neighbouring the nitrogen atoms were resonated at 2.51 ppm. Finally, the protons on the carbon adjacent to the acrylate carbonyl groups were observed at 2.78 ppm. Moreover, the absence of any signal at around 5.8–6.6 ppm which correspond to the acrylate double bond protons (CH_2 =CH–) clearly proves that the synthesized PDD is pure. The integral ratios were calculated and were found to be in good accordance with the structure of the synthesized PDD.

Similarly, the structure of PAMCO was characterized by FTIR and NMR spectroscopy. The FTIR spectrum of PAMCO is given in Fig. 6 along with azidoethanol and neat CO. The characteristic carbonyl and hydroxyl vibration bands of CO were observed at 1743 and 3386 cm^{-1}, respectively (Mülazim et al., 2013). The bands observed at around 2855 and 2925 cm^{-1} were attributed to the symmetric and asymmetric –CH stretching vibrations. After the reaction of CO with $POCl_3$ and azidoethanol, the intensity of the hydroxyl band declined and new peaks appeared in the spectrum of PAMCO. The band at 2100 cm^{-1} in the spectrum of PAMCO is due to the characteristic azide stretching vibrations. Moreover, the bands at 1020 and 940 cm^{-1} were attributed to the newly formed phosphate ester groups (Jia et al., 2016, 2015).

The ^{1}H NMR spectra of neat CO and PAMCO are presented in Fig. 7. The aliphatic protons of the fatty acid chains in neat CO were resonated between 0.88 and 2.32 ppm as can be seen from the ^{1}H NMR spectrum of CO. The methylene (–CH_2) protons (b) of the glycerol unit in CO were resonated at 4.1–4.3 ppm while the –CH proton (a) in the glycerol unit was detected at 5.27 ppm. The double bond protons (h) were resonated at 5.6–5.4 ppm. The characteristic peak of the proton adjacent to the

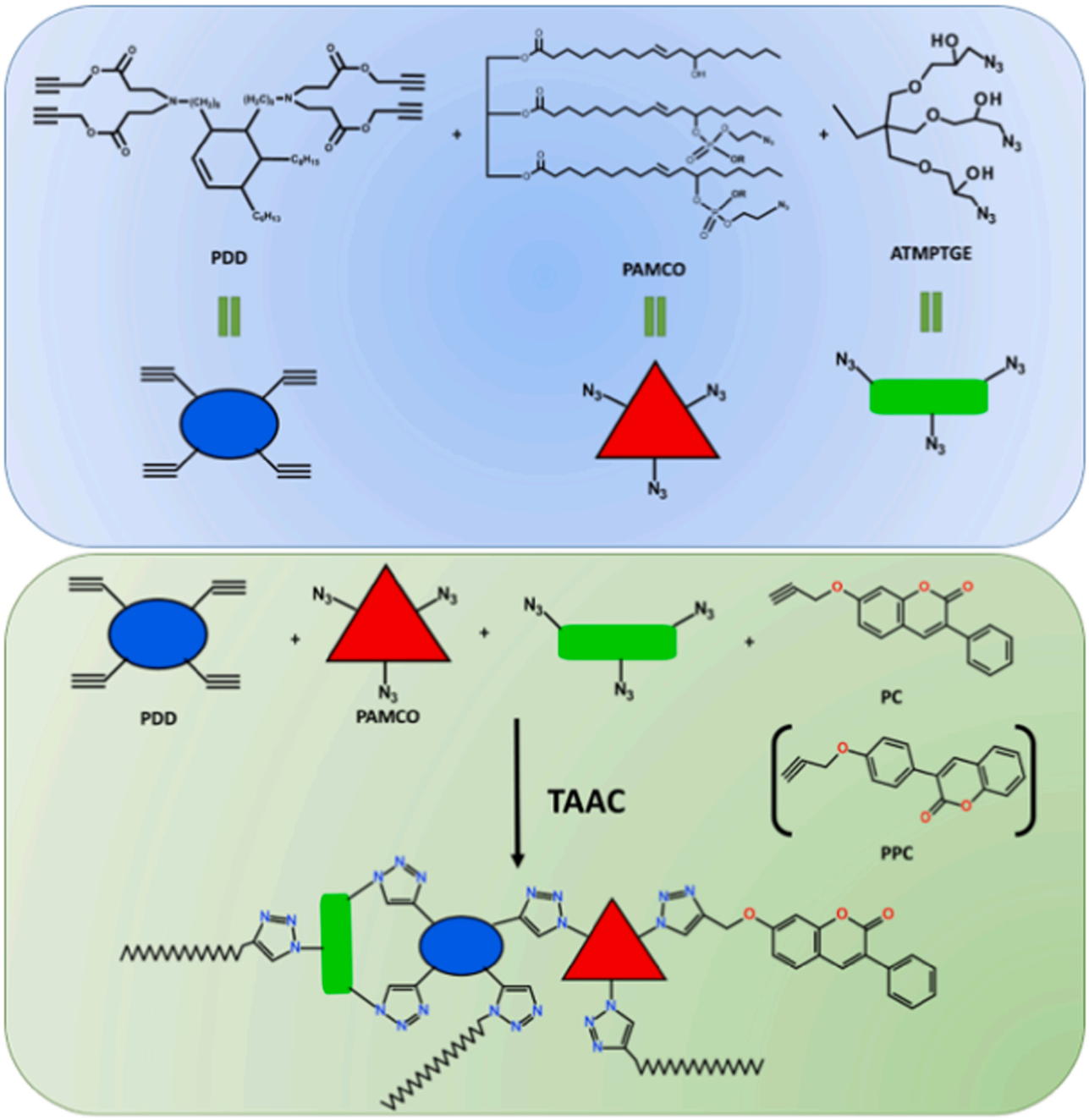

Scheme 4. The synthetic route to TAAC cured bio-based elastomeric thermosets.

–OH group (f) was observed at 3.62 ppm. After phosphorylation and the introduction of azide groups, the intensity of this peak at 3.62 ppm decreased as can be seen from the spectrum of PAMCO. A new peak appeared at 2.49 ppm in this spectrum was ascribed to the –C**H**–OP=O- protons (k) (Jia et al., 2015). The protons adjacent to the azide functionality were detected at 3.49 ppm (l) and the other neighbouring protons –OC**H**$_2$CH$_2$N$_3$ (m), were found to resonate at around 4.35 which partially overlapped with methylene protons of glycerol in PAMCO. These peaks are in good accordance with the literature (Daglar et al. 2021). These results prove that the phosphorous and azide functionalities were successfully introduced to CO. Moreover, the PAMCO was characterized by ^{31}P NMR (Fig. 7 C). The ^{31}P NMR of PAMCO displayed two peaks. The peak at − 0.45 was attributed to the monosubstituted derivative (–OPO(OCH$_2$CH$_2$N$_3$)OH) while the other peak at − 1.93 ppm was ascribed to the double substituted phosphate ester groups (–OPO (OCH$_2$CH$_2$N$_3$)$_2$). These observed peaks are in good accordance with similar phosphate esters in the literature (Przybylak et al., 2021; Changi et al., 2012; Howell and Ostrander, 2019). In the first step of the reaction most of the –OH groups were reacted with POCl$_3$ to give –OPOCl$_2$ groups on CO. Then, as it is understood from the ^{31}P NMR spectrum, only a portion of the –OPOCl$_2$ groups were reacted with azidoethanol and the remaining –OPO(OCH$_2$CH$_2$N$_3$)Cl groups were hydrolyzed during the washing steps to –OPO(OCH$_2$CH$_2$N$_3$)OH. Moreover, the absence of any peak in the P NMR spectrum of PAMCO over 0 ppm, proves that all chlorine groups were removed. For instance; when, –OPOCl$_2$ groups were generated on CO, the oil exhibited a P NMR signal at 20 ppm (Jia et al. 2015). Thus, based on these findings it can be concluded that PAMCO was synthesized successfully.

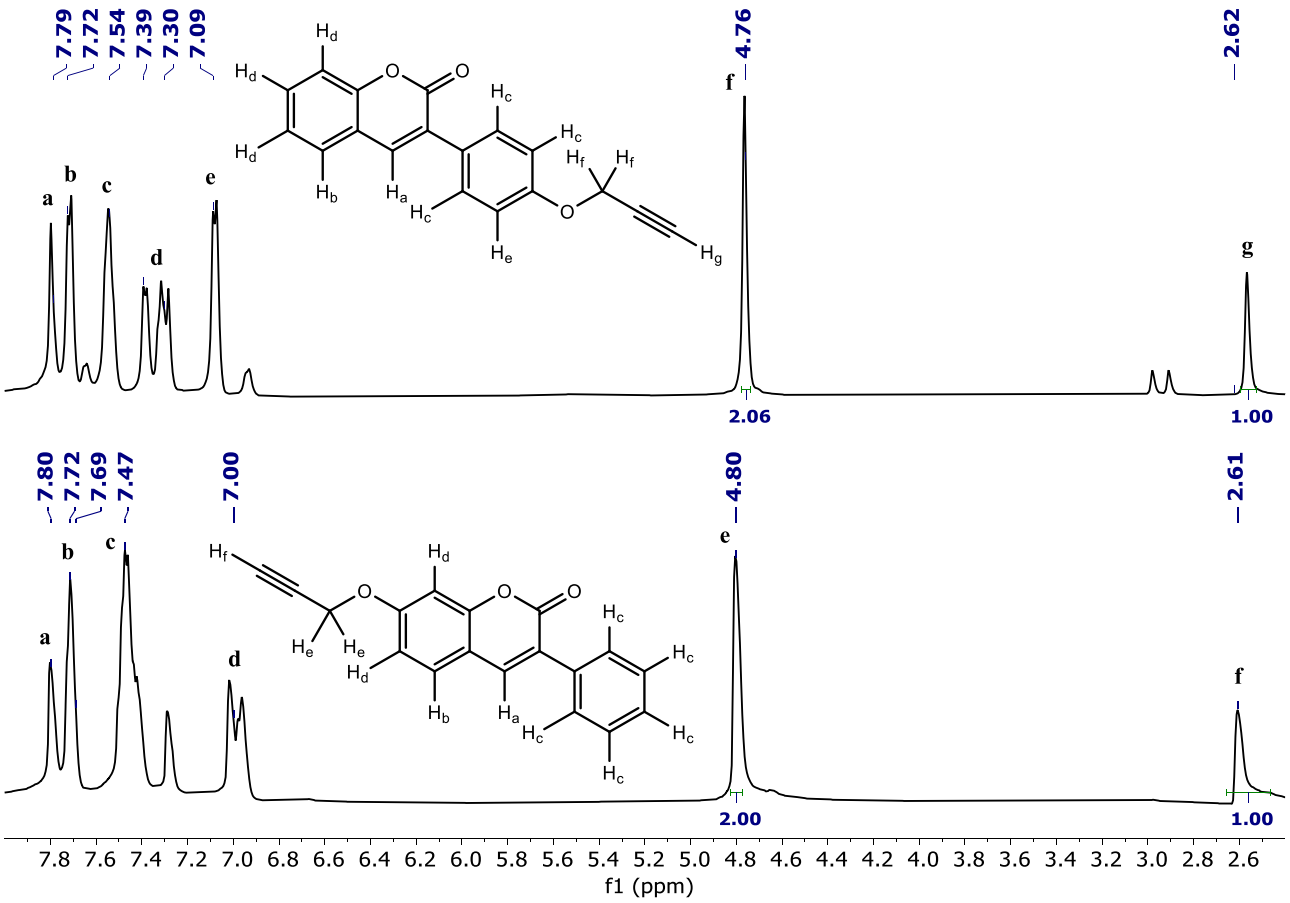

Fig. 2. ^{1}H NMR spectra of PC and PPC.

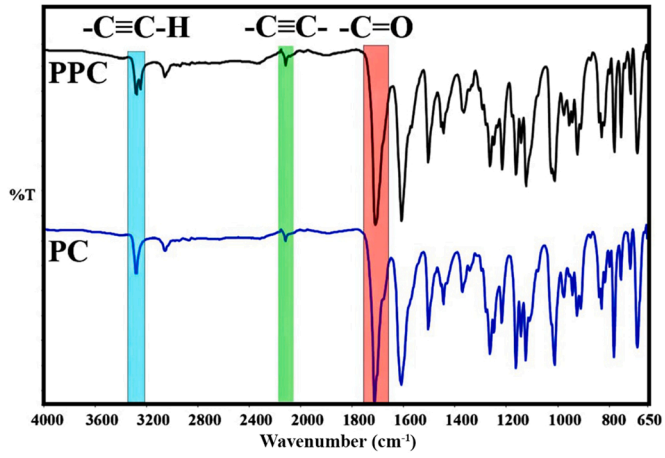

Fig. 3. FTIR spectra of PC and PPC.

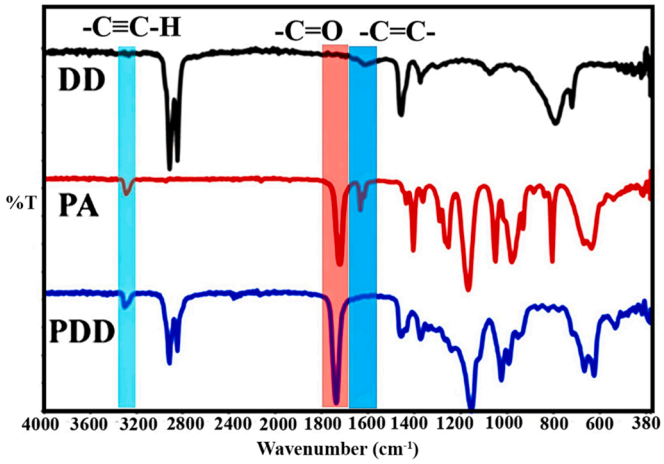

Fig. 4. FTIR spectra of DD, PA and PDD.

3.2. Structural characterization of the thermally cured thermosets

In this work, thermoset materials were prepared by using azidated CO and propargylated dimer diamine with the aid of ATMPTGE. When ATMPTGE was not used, we could not be able to produce self-standing films from only PAMCO and PDD, instead highly viscous rubber-like masses were obtained. Nevertheless, we manage to keep the total ratio of ATMPTGE at 15% with respect to the total weight to have a high amount of renewable content.

The structural characterization of the bio-based networks was performed by FTIR spectroscopy. The FTIR spectra of the films are given in Fig. 8. All the obtained films displayed similar spectra. The bands between 3600 and 3400 cm^{-1} were due to the –OH stretching vibrations of the ATMPTGE. The characteristic carbonyl stretching bands were detected at around 1730 cm^{-1} while the bands between 2920 and 2850 cm^{-1} were attributed to the aliphatic –CH groups. When coumarins were incorporated the carbonyl bands were expanded due to the overlapping of the bands of the carbonyls of the vegetable oil based monomers and coumarins. Additionally, new peaks appeared at around 1600 cm^{-1} in the spectra of the coumarin-containing samples corresponding to the aromatic –C═C– stretching vibrations. We must note that in all spectra a weak band at around 2100 cm^{-1} was detected which

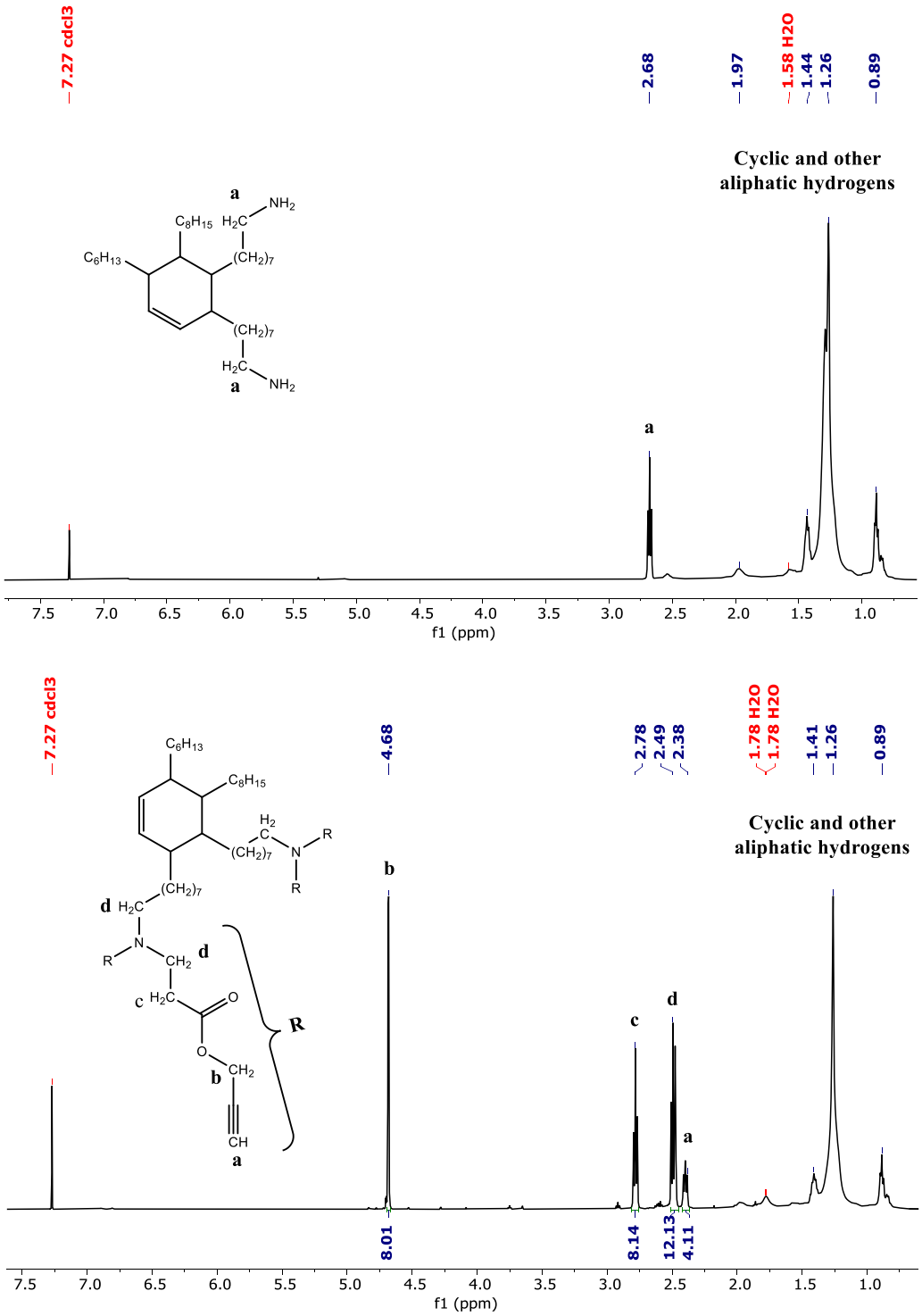

Fig. 5. ^{1}H NMR spectra of neat DD (top) and PDD (below).

indicates that the azide groups were not completely reacted. This situation was also encountered previously in literature (Han et al., 2016; Xu et al., 2016; Besset et al., 2010; Lutz, 2008; Hong et al., 2013).

Moreover, we determined the gel content values of the crosslinked bio-based networks and the gel content values were found as 74%, 79%, 80%, 83% and 87% for DPA, DPA–PC10, DPA–PC20, DPA–PC10 and DPA–PPC20, respectively. According to these results it can be said that monofunctional coumarin derivatives were effective towards TAAC reactions and when their amount was increased in the formulations the gel content values also increased. The gel content value of DPA was found to be relatively low which could be ascribed to the steric effects arising from the long alkyl chains of the fatty acids.

3.3. Mechanical properties

The mechanical properties of the TAAC cured thermosets were evaluated by measuring their tensile strengths. The representative tensile curves of the thermosets are presented in Fig. 9 and the average tensile strength and elongation at break values are listed in Table 2. Note that the values given in Table 2 are average values of at least three

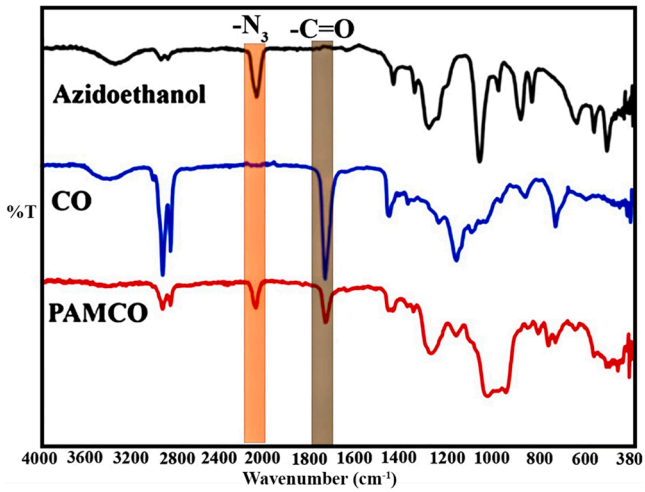

Fig. 6. FTIR spectra of azidoethanol, CO and PAMCO.

different specimens. The thermosets displayed very low tensile strengths and high elongation at break values thus they behaved like elastomers. These findings are in good accordance with the study of Yuan et al. (2018). Contrary to the decreased crosslinking, the addition of the monofunctional coumarins led to an increase in the tensile strengths while decreasing the elongation percentages. This situation can be explained by the rigid aromatic structures of the novel coumarins and also it might be attributed to interactions like π-π stacking of the aromatic units or H-bonding ability of the carbonyl groups of the coumarins.

3.4. Thermal properties

The thermal stability of the thermosets was investigated by TGA under a nitrogen atmosphere. Figs. 10a and 10b display the TGA curves and the corresponding derivative weight curves. The results of the thermal analysis are collected in Table 2. All samples displayed similar thermal decomposition behaviors. The 5% weight loss temperatures were found to be above 200 °C and these weight losses were attributed to the unreacted monomers and residual solvent confined within the polymer matrix. All thermosets displayed two main degradation steps over 340 °C however, DPA encoded samples displayed an additional degradation step at around 260 °C. The incorporation of coumarins led to a slight increase in the T_1 values while the T_2 temperatures slightly declined with PC, PPC improved the T_2 values. Even though the rigid coumarin rings increased the thermal decomposition temperatures, the decreased crosslinking led to a decrease in the obtained char yields. When compared, PC was found to be less thermally stable than PPC in their corresponding thermosets.

In the work of Yuan et al., in which alkyne-functionalized lignin and azide-functionalized fatty acid derivatives were used, the onset of decomposition temperatures (5% weight loss) was found to be 280 °C and the obtained char yields were below 5% at 700 °C (Yuan et al. 2018). According to the char yields in this work and that of Yuan et al., it can be said that these phosphorylated CO-containing thermosets are superior in terms of thermal stability despite the fact the 5% weight loss temperatures were lower in this work. The early degradation of the thermosets prepared herein can be attributed to the well-known early decomposition of the phosphorus-containing agents.

Glass transition temperatures (Tg) of the thermosets were determined by DSC measurements. The Tg values are collected in Table 2. The DPA encoded films displayed a Tg value of 3.3 °C. When coumarins were added the Tg values increased in spite of the decreased crosslinking density and this result could be ascribed to the steric hindrance induced by the presence of the rigid and bulky aromatic coumarin rings as side

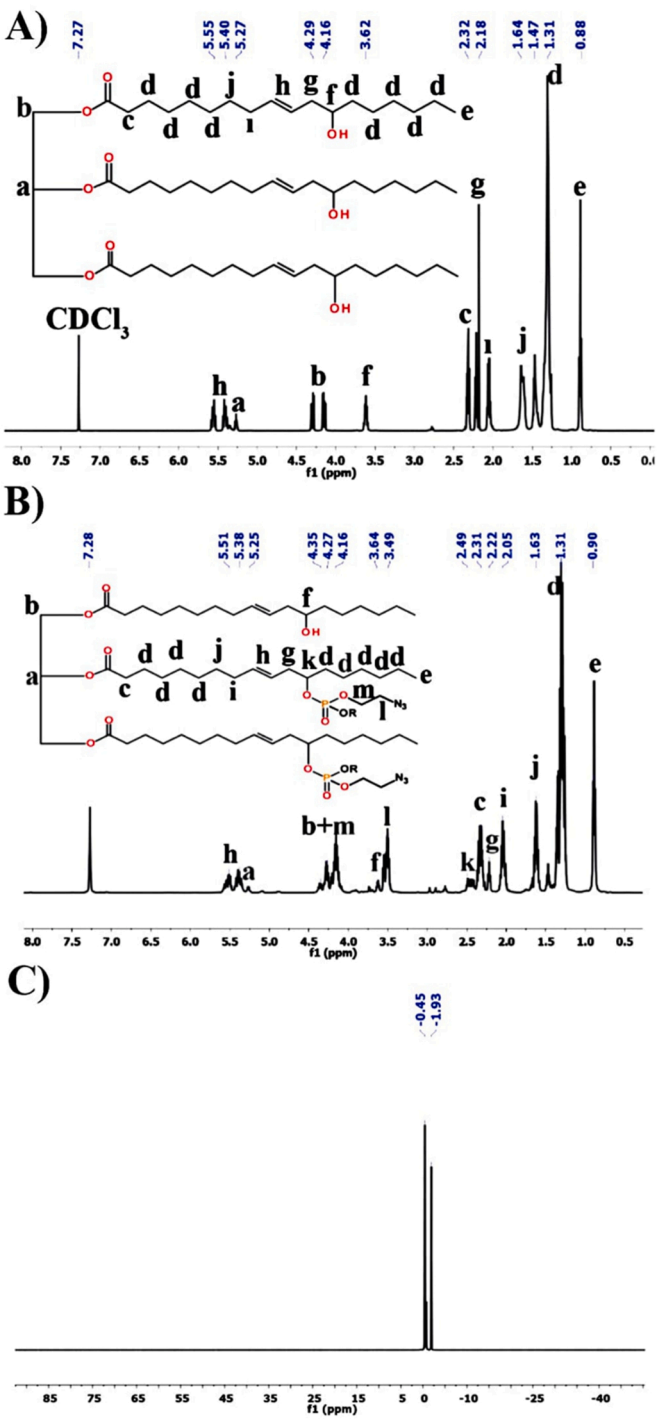

Fig. 7. ^{1}H NMR of CO (a), PAMCO (b) and P NMR of PAMCO (c).

chain constituents. However, a trend was not observed in the Tgs. When the amount of PC was increased from 10% to 20%, the Tg value was decreased, whereas in the same situation the PPC led to an increase in the Tg value.

3.5. Wettability

The water repellency performance of materials generally depends on two factors; the surface energy and the surface roughness. In many studies in literature, to prepare hydrophobic coatings; fluorinated or siloxane-based compounds are widely used due to their low surface energy (Daglar et al., 2020) and silica nanoparticles are also used to

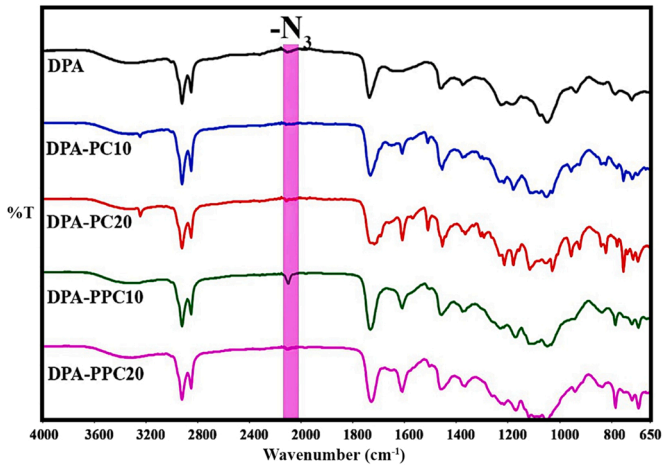

Fig. 8. FTIR spectra of the TAAC cured networks.

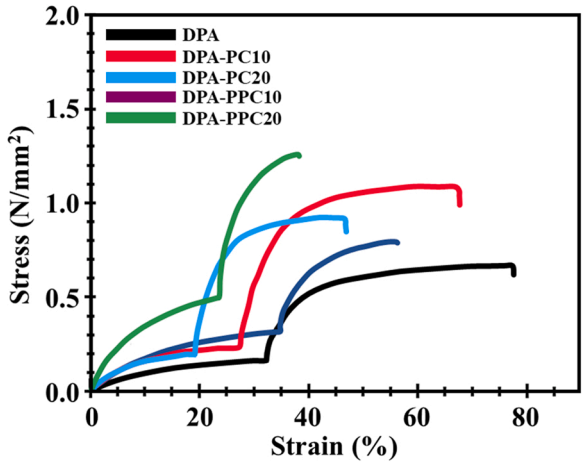

Fig. 9. Representative stress-strain curves of the TAAC cured thermosets.

Table 2
Thermal and mechanical properties of the thermosets.

	Tensile Strength (MPa)	Elongation at break (%)	T_1[a] (°C)	T_2[a]	Char (%)	Tg (°C)
DPA	0.13	84 ± 8	260/ 342	476	13.8	3.3
DPA–PC10	0.19	68 ± 9	350	470	8.84	7.3
DPA–PC20	0.18	45 ± 11	346	470	7.74	5.4
DPA–PPC10	0.25	52 ± 9	353	481	11.8	4.3
DPA–PPC20	0.46	39 ± 12	359	480	12.5	9.5

[a] T_1 and T_2 are the maximum weight loss temperatures, which were determined from the maximum of the corresponding derivative curves.

increase the surface roughness (Şeker and Çakmakçi, 2020). Vegetable oils are good canditates due to their low surface energy and inherent water repellency but adding polar constituents could lead to a decline in water repellent properties. For example, tung oil was previously cured under UV light in the presence of a cationic photoinitiator and due to oxidative curing polar species such as –OH, -OOH, -COOH, formed and the coatings displayed a WCA of 66° (Şeker and Çakmakçi, 2020).

Since the TAAC cured networks are vegetable-based, it can be expected from them to be water repellent. However, the polar triazole rings, unreacted free azide groups as well as the hydroxyl groups of ATMPTGE led to polar surfaces (Fig. 11). The addition of monofunctional coumarins contributed to the polarity and thus the WCA values declined. Interestingly, the decrease in the WCA was much more pronounced in PPC-containing thermosets.

3.6. Antibacterial properties

The antibacterial activity of the vegetable based thermosets was tested against both gram-positive (*S. aureus*) and gram-negative (*E. coli*) bacteria by measuring their diameter of inhibition zones. The inhibition zone diameters of the TAAC cured samples are given in Table 3.

Previously, the antibacterial activities of several coumarins were investigated (Abd El-Fattah et al., 2017; Kayser and Kolodziej, 1999; De Souza et al., 2005). The antibacterial activity of coumarins stems from their lipophilic character and their planar molecular geometry which enables its penetration through the bacterial cell walls (de Souza et al., 2005). The functional groups around the aromatic ring of a simple coumarin structure affects its antibacterial activity against gram-positive and gram-negative bacteria. Studies on coumarin derivatives revealed that especially the dimethoxy-substituted ones are effective againts fungal strains and bacteria due to the increased lipophilicity, leading to ease of penetration (Kayser and Kolodziej, 1999; Céspedes et al., 2006). Thus, the antibacterial activity of coumarins strongly depend on their structure. Triazole derivatives are also known for their antibacterial activity (Strzelecka and Świątek, 2021). Thus, in this work a unique combination of antibacterial triazole groups with coumarin takes place.

Abd El-Fattah et al. (2017) synthesized thiazole ring-containing coumarins and incorporated them into polyurethane-based coatings. But it must be noted that the coumarin derivatives were not bounded to the polyurethane matrix, thus they were released during the antibacterial test and this led to high zone inhibition diameters ranging from 21 to 42 mm depending on the coumarin structure and its concentration in the polyurethane matrix.

Based on the antibacterial test results the DPA was found to be inactive against bacteria. However, the addition of the coumarin species led to antibacterial activity. PC-containing thermosets were found to be much more efficient in killing the bacteria than the PPC-containing ones. In the case of PC, propargyl group thus the triazole group is directly bonded to the coumarin's phenyl moiety and another phenyl group is attached at position 3 in the coumarin. On the other hand, in PPC, the propargyl group is attached to the phenyl group which is then connected to the coumarin ring. Thus, the triazole group and the coumarin ring are separated by the phenyl group. The reason for the relatively lower antibacterial activity could be ascribed to this difference. Moreover, it can be said that the phenyl ring in the structure of PC increases its lipophilicity which further contributes to the antibacterial activity.

4. Conclusions

In this study, coumarin-containing, dimer diamine and CO-based antibacterial thermosets were prepared via TAAC polymerization. Two novel, vegetable oil-based oligomers were prepared for the first time in literature. Phosphorus and azide functionalized CO was prepared in two steps in one pot. Propargylated dimer diamine was synthesized via aza-Michael reaction. The thermosets displayed low tensile strength values and high elongation at break values. The use of phosphorylated CO resulted in improved thermal properties and high char yields. The incorporation of coumarin species into these vegetable oil-based thermosets resulted in antibacterial properties. Thus, we successfully prepared antibacterial thermosets via metal-free azide-alkyne click chemistry.

Finally, we believe that this study will inspire researchers for the synthesis and development of phosphorus-containing thermally stable and antibacterial thermoset materials from renewable and sustainable resources.

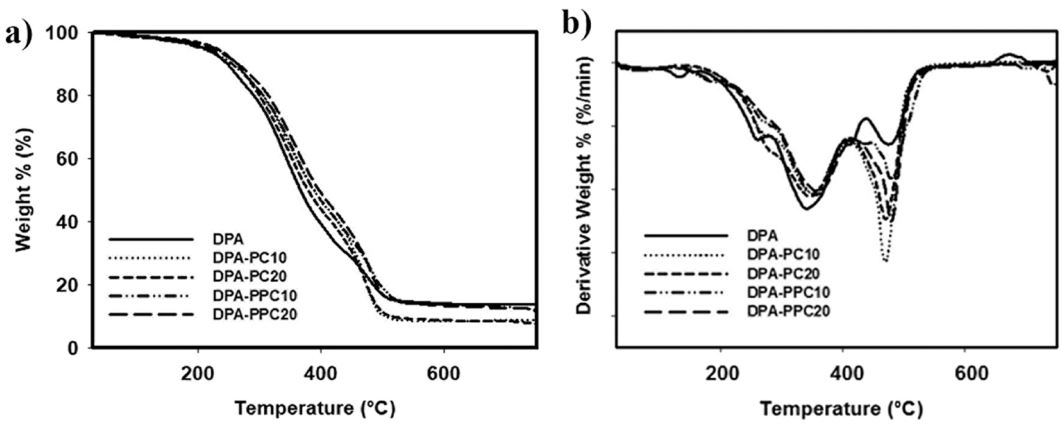

Fig. 10. TGA curves (a) and the derivative weight curves of the thermosets (b).

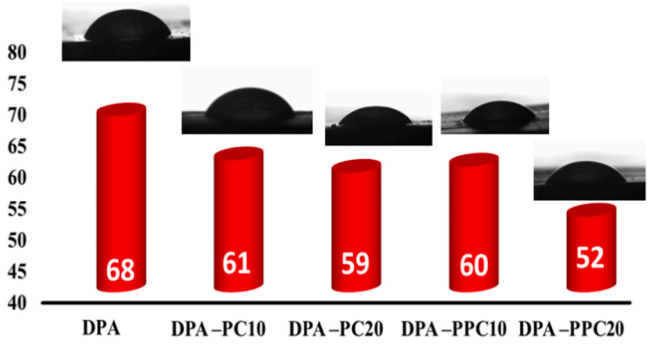

Fig. 11. WCA values of the vegetable oil-based thermosets.

Table 3
Inhibition zone diameters of the thermosets.

	E. coli (mm)	*S. aureus* (mm)
DPA	–	–
DPA–PC10	9	10
DPA–PC20	11	11
DPA–PPC10	4	6
DPA–PPC20	8	10

CRediT authorship contribution statement

Emrah Çakmakçi: Investigation, Conceptualization, Writing - original draft **Mücahit Özdemir**: Investigation, Data curation, Writing – original draft **Ferhat Şen:** Investigation, Writing – review & editing. **Mustafa Bulut:** Conceptualization, Writing – review & editing. **Bahattin Yalçin:** Supervision, Writing – review & editing.

Declaration of Competing Interest

The authors declare that they have no known competing financial interests or personal relationships that could have appeared to influence the work reported in this paper.

References

Abd El-Fattah, M., Abd El-Wahab, H., Bashandy, M., El-Eisawy, R., Abd El-Hai, F., Saeed, M., 2017. Potential application of some coumarin derivatives incorporated thiazole ring as ecofriendly antimicrobial, flame retardant and corrosion inhibitor additives for polyurethane coating. Prog. Org. Coat. 111, 57–66. https://doi.org/10.1016/j.porgcoat.2017.05.005.

Abdallah, M., Hijazi, A., Graff, B., Fouassier, J.-P., Rodeghiero, G., Gualandi, A., et al., 2019. Coumarin derivatives as versatile photoinitiators for 3D printing, polymerization in water and photocomposite synthesis. Polym. Chem. 10, 872–884. https://doi.org/10.1039/C8PY01708E.

Agnaou, R., Capelot, M., Tence-Girault, S., Tournilhac, F., Leibler, L., 2014. Supramolecular thermoplastic with 0.5 Pa·s melt viscosity. J. Am. Chem. Soc. 136, 11268–11271. https://doi.org/10.1021/ja505956z.

Alam, M., Alandis, N.M., 2014. Corn oil based poly (ether amide urethane) coating material—synthesis, characterization and coating properties. Ind. Crops Prod. 57, 17–28. https://doi.org/10.1016/j.indcrop.2014.03.023.

Alam, M., Akram, D., Sharmin, E., Zafar, F., Ahmad, S., 2014. Vegetable oil based eco-friendly coating materials: a review article. Arab. J. Chem. 7, 469–479. https://doi.org/10.1016/j.arabjc.2013.12.023.

Arévalo, M.J., López, Ó., Gil, M.V., 2016. Green chemical synthesis and click reactions. in: srinivasan chandrasekaran. Click Reactions in Organic Synthesis. Wiley-VCH Verlag GmbH&amp. Co. KGaA., Weinheim, Germany, pp. 77–97. https://doi.org/10.1002/9783527694174.ch3.

Auvergne, R., Caillol, S., David, G., Boutevin, B., Pascault, J.-P., 2014. Biobased thermosetting epoxy: present and future. Chem. Rev. 114, 1082–1115. https://doi.org/10.1021/cr3001274.

Besset, C., Bernard, J., Fleury, E., Pascault, J.-P., Cassagnau, P., Drockenmuller, E., et al., 2010. Bio-sourced networks from thermal polyaddition of a starch-derived α-azide-ω-alkyne AB monomer with an A2B2 aliphatic cross-linker. Macromolecules 43, 5672–5678. https://doi.org/10.1021/ma100770t.

Besset, C., Pascault, J.-P., Fleury, E., Drockenmuller, E., Bernard, J., 2010. Structure–properties relationship of biosourced stereocontrolled polytriazoles from click chemistry step growth polymerization of diazide and dialkyne dianhydrohexitols. Biomacromolecules 11, 2797–2803. https://doi.org/10.1021/bm100872h.

Beyler-Çiğil, A., Birtane, H., Şen, F., Kahraman, M.V., 2021. Transparent and flexible antibacterial photocrosslinked thin films against the S. aureus and E. coli pathogen bacteria. Mater. Today Commun. 27, 102463 https://doi.org/10.1016/j.mtcomm.2021.102463.

Birtane, H., Şen, F., Bozdağ, B., Kahraman, M.V., 2021. Antibacterial UV-photocured acrylic coatings containing quaternary ammonium salt. Polym. Bull. 78, 3577–3588. https://doi.org/10.1007/s00289-020-03287-0.

Borges, F., Roleira, F., Milhazes, N., Santana, L., Uriarte, E., 2005. Simple coumarins and analogues in medicinal chemistry: occurrence, synthesis and biological activity. Curr. Med. Chem. 12, 887–916. https://doi.org/10.2174/0929867053507315.

Cakmakci, E., Sen, F., Kahraman, M.V., 2019. Isosorbide diallyl based antibacterial thiol–ene photocured coatings containing polymerizable fluorous quaternary phosphonium salt. ACS Sustain. Chem. Eng. 7, 10605–10615. https://doi.org/10.1021/acssuschemeng.9b01161.

Çalgeris, İ., Çakmakçı, E., Ogan, A., Kahraman, M.V., Kayaman-Apohan, N., 2012. Preparation and drug release properties of lignin–starch biodegradable films. Starch-Stärke 64, 399–407. https://doi.org/10.1002/star.201100158.

Céspedes, C.L., Avila, J.G., Martínez, A., Serrato, B., Calderón-Mugica, J.C., Salgado-Garciglia, R., 2006. Antifungal and antibacterial activities of Mexican tarragon (Tagetes lucida). J. Agric. Food Chem. 54, 3521–3527. https://doi.org/10.1021/jf053071w.

Changi, S., Matzger, A.J., Savage, P.E., 2012. Kinetics and pathways for an algal phospholipid (1, 2-dioleoyl-sn-glycero-3-phosphocholine) in high-temperature (175–350 °C) water. Green. Chem. 14, 2856–2867. https://doi.org/10.1039/C2GC35639B.

Chen, C.-H., Tung, S.-H., Jeng, R.-J., Abu-Omar, M.M., Lin, C.-H., 2019. A facile strategy to achieve fully bio-based epoxy thermosets from eugenol. Green Chem. 21, 4475–4488. https://doi.org/10.1039/C9GC01184F.

Chen, Q., Yang, Q., Gao, P., Chi, B., Nie, J., He, Y., 2019. Photopolymerization of coumarin-containing reversible photoresponsive materials based on wavelength selectivity. Ind. Eng. Chem. Res. 58, 2970–2975. https://doi.org/10.1021/acs.iecr.8b05164.

Daglar, O., Cakmakci, E., Gunay, U.S., Hizal, G., Tunca, U., Durmaz, H., 2020. A straightforward method for fluorinated polythioether synthesis. Macromolecules 53, 2965–2975. https://doi.org/10.1021/acs.macromol.0c00548.

Daglar, O., Çakmakçi, E., Gunay, U.S., Hizal, G., Tunca, U., Durmaz, H., 2021. Acetylene dicarboxylic acid diallyl ester: a versatile monomer for thiol–ene photocured networks. Macromol. Mater. Eng. 306, 2100427. https://doi.org/10.1002/mame.202100427.

De Souza, S.M., Delle Monache, F., Smânia, A., 2005. Antibacterial activity of coumarins. Z. Naturforsch. C 60, 693–700. https://doi.org/10.1515/znc-2005-9-1006.

Feng, Y., Liang, H., Yang, Z., Yuan, T., Luo, Y., Li, P., et al., 2017. A solvent-free and scalable method to prepare soybean-oil-based polyols by thiol–ene photo-click reaction and biobased polyurethanes therefrom. ACS Sustain. Chem. Eng. 5, 7365–7373. https://doi.org/10.1021/acssuschemeng.7b01672.

Fernández-Francos, X., Konuray, A.-O., Belmonte, A., De La Flor, S., Serra, À., Ramis, X., 2016. Sequential curing of off-stoichiometric thiol–epoxy thermosets with a custom-tailored structure. Polym. Chem. 7, 2280–2290. https://doi.org/10.1039/C6PY00099A.

Froidevaux, V., Negrell, C., Caillol, S., Pascault, J.-P., Boutevin, B., 2016. Biobased amines: from synthesis to polymers; present and future. Chem. Rev. 116, 14181–14224. https://doi.org/10.1021/acs.chemrev.6b00486.

Gandini, A., Lacerda, T.M., 2015. From monomers to polymers from renewable resources: recent advances. Prog. Polym. Sci. 48, 1–39. https://doi.org/10.1016/j.progpolymsci.2014.11.002.

Gupta, S., Ameta, C., Ameta, R., Punjabi, P.B., 2020. Click chemistry: a tool for green chemical organic synthesis. In: Boddula, I.R., Asiri, A.M. (Eds.), Green Sustainable Process for Chemical and Environmental Engineering and Science. Elsevier Inc, pp. 13–48. https://doi.org/10.1016/B978-0-12-819539-0.00002-6.

Han, Y., Yuan, L., Li, G., Huang, L., Qin, T., Chu, F., et al., 2016. Renewable polymers from lignin via copper-free thermal click chemistry. Polymer 83, 92–100. https://doi.org/10.1016/j.polymer.2015.12.010.

Harvey, B.G., Guenthner, A.J., Meylemans, H.A., Haines, S.R., Lamison, K.R., Groshens, T.J., et al., 2015. Renewable thermosetting resins and thermoplastics from vanillin. Green. Chem. 17, 1249–1258. https://doi.org/10.1039/C4GC01825G.

He, M., Jiang, S., Xu, R., Yang, J., Zeng, Z., Chen, G., 2014. Facile functionalization of soybean oil by thiol-ene photo-click reaction for the synthesis of polyfunctional acrylate. Prog. Org. Coat. 77, 868–871. https://doi.org/10.1016/j.porgcoat.2014.01.018.

Hong, J., Shah, B.K., Petrović, Z.S., 2013. Vegetable oil cast resins via click chemistry: effects of cross-linkers. Eur. J. Lipid Sci. Technol. 115, 55–60. https://doi.org/10.1002/ejlt.201200143.

Howell, B.A., Ostrander, E.A., 2019. Thermal degradation of flame-retardant compounds derived from castor oil. J. Therm. Anal. Calorim. 138, 3961–3975. https://doi.org/10.1007/s10973-019-08355-w.

Hoyle, C.E., Lowe, A.B., Bowman, C.N., 2010. Thiol-click chemistry: a multifaceted toolbox for small molecule and polymer synthesis. Chem. Soc. Rev. 39, 1355–1387. https://doi.org/10.1039/B901979K.

Hu, Y., Wang, B., Yang, J., Liu, T., Sun, J., Wang, X., 2019. Synthesis and biological evaluation of 3-arylcoumarin derivatives as potential anti-diabetic agents. J. Enzym. Inhib. Med. Chem. 34, 15–30. https://doi.org/10.1080/14756366.2018.1518958.

Ionescu, M., Radojčić, D., Wan, X., Petrović, Z.S., Upshaw, T.A., 2015. Functionalized vegetable oils as precursors for polymers by thiol-ene reaction. Eur. Polym. J. 67, 439–448. https://doi.org/10.1016/j.eurpolymj.2014.12.037.

Jia, P., Zhang, M., Hu, L., Bo, C., Zhou, Y.-h, 2015. Synthesis, application, and flame-retardant mechanism of a novel phosphorus-containing plasticizer based on castor oil for polyvinyl chloride. J. Therm. Anal. Calorim. 120, 1731–1740. https://doi.org/10.1007/s10973-015-4540-1.

Jia, P., Zhang, M., Liu, C., Hu, L., Feng, G., Bo, C., et al., 2015. Effect of chlorinated phosphate ester based on castor oil on thermal degradation of poly (vinyl chloride) blends and its flame retardant mechanism as secondary plasticizer. RSC Adv. 5, 41169–41178. https://doi.org/10.1039/C5RA05784A.

Jia, P., Hu, L., Zhang, M., Zhou, Y.-h, 2016. TG-FTIR and TG-MS analysis applied to study the flame retardancy of PVC–castor oil-based chlorinated phosphate ester blends. J. Therm. Anal. Calorim. 124, 1331–1339. https://doi.org/10.1007/s10973-015-5199-3.

Kargarfard, N., Diedrich, N., Rupp, H., Döhler, D., Binder, W.H., 2018. Improving kinetics of “click-crosslinking” for self-healing nanocomposites by graphene-supported Cu-nanoparticles. Polymers 10, 17. https://doi.org/10.3390/polym10010017.

Kayser, O., Kolodziej, H., 1999. Antibacterial activity of simple coumarins: structural requirements for biological activity. Z. Naturforsch. C 54, 169–174. https://doi.org/10.1515/znc-1999-3-405.

Kolb, H.C., Finn, M., Sharpless, K.B., 2001. Click chemistry: diverse chemical function from a few good reactions. Angew. Chem. Int. Ed. 40, 2004–2021. https://doi.org/10.1002/1521-3773(20010601)40:11<2004::AID-ANIE2004>3.0.CO;2-5.

Lutz, J.F., 2008. Copper-free azide–alkyne cycloadditions: new insights and perspectives. Angew. Chem. Int. Ed. 47, 2182–2184. https://doi.org/10.1002/anie.200705365.

Ma, S., Liu, X., Jiang, Y., Tang, Z., Zhang, C., Zhu, J., 2013. Bio-based epoxy resin from itaconic acid and its thermosets cured with anhydride and comonomers. Green. Chem. 15, 245–254. https://doi.org/10.1039/C2GC36715G.

Mülazim, Y., Çakmakçı, E., Kahraman, M.V., 2011. Preparation of photo curable highly hydrophobic coatings using a modified castor oil derivative as a sol–gel component. Prog. Org. Coat. 72, 394–401. https://doi.org/10.1016/j.porgcoat.2011.05.012.

Mülazim, Y., Çakmakçı, E., Kahraman, M.V., 2013. Photo-curable highly water-repellent nanocomposite coatings. J. Vinyl Addit. Technol. 19, 31–38. https://doi.org/10.1002/vnl.20309.

Pansumdaeng, J., Kuntharin, S., Harnchana, V., Supanchaiyamat, N., 2020. Fully bio-based epoxidized soybean oil thermosets for high performance triboelectric nanogenerators. Green. Chem. 22, 6912–6921. https://doi.org/10.1039/D0GC01738H.

Przybylak, M., Dutkiewicz, M., Szubert, K., Maciejewski, H., Rojewski, S., 2021. Multifunctional cotton fabrics obtained by modification with silanes containing esters of phosphoric acid as substituents. Materials 14, 1542. https://doi.org/10.3390/ma14061542.

Şeker, H., Çakmakçi, E., 2020. Fully bio-based thiol-ene photocured thermosets from isosorbide and tung oil. J. Polym. Sci. 58, 1105–1114. https://doi.org/10.1002/pol.20190291.

Şen, F., Kahraman, M.V., 2018. Preparation and characterization of hybrid cationic hydroxyethyl cellulose/sodium alginate polyelectrolyte antimicrobial films. Polym. Adv. Technol. 29, 1895–1901. https://doi.org/10.1002/pat.4298.

Şen, F., Uzunsoy, İ., Baştürk, E., Kahraman, M.V., 2017. Antimicrobial agent-free hybrid cationic starch/sodium alginate polyelectrolyte films for food packaging materials. Carbohydr. Polym. 170, 264–270. https://doi.org/10.1016/j.carbpol.2017.04.079.

Singh, M.S., Chowdhury, S., Koley, S., 2016. Advances of azide-alkyne cycloaddition-click chemistry over the recent decade. Tetrahedron 72, 5257–5283. https://doi.org/10.1016/j.tet.2016.07.044.

Strzelecka, M., Świątek, P., 2021. 1, 2, 4-triazoles as important antibacterial agents. Pharmaceuticals 14, 224. https://doi.org/10.3390/ph14030224.

Tasdelen, M.A., Yagci, Y., 2013. Light-induced click reactions. Angew. Chem. Int. Ed. 52, 5930–5938. https://doi.org/10.1002/anie.201208741.

Tunca, U., 2018. Click and multicomponent reactions work together for polymer chemistry. Macromol. Chem. Phys. 219, 1800163. https://doi.org/10.1002/macp.201800163.

Uemura, Y., Shimasaki, T., Teramoto, N., Shibata, M., 2016. Thermal and mechanical properties of bio-based polymer networks by thiol-ene photopolymerizations of gallic acid and pyrogallol derivatives. J. Polym. Res. 23, 1–10. https://doi.org/10.1007/s10965-016-1105-3.

Xu, L.Q., Pranantyo, D., Neoh, K.-G., Kang, E.-T., Teo, S.L.-M., Fu, G.D., 2016. Antifouling coatings based on covalently cross-linked agarose film via thermal azide-alkyne cycloaddition. Colloids Surf. B 141, 65–73. https://doi.org/10.1016/j.colsurfb.2016.01.024.

Yuan, L., Zhang, Y., Wang, Z., Han, Y., Tang, C., 2018. Plant oil and lignin-derived elastomers via thermal azide–alkyne cycloaddition click chemistry. ACS Sustain. Chem. Eng. 7, 2593–2601. https://doi.org/10.1021/acssuschemeng.8b05617.

Zhang, X., Xi, W., Wang, C., Podgórski, M., Bowman, C.N., 2016. Visible-light-initiated thiol-michael addition polymerizations with coumarin-based photobase generators: another photoclick reaction strategy. ACS Macro Lett. 5, 229–233. https://doi.org/10.1021/acsmacrolett.5b00923.